ORIGINAL PAPER

Thermoplastic Blends Based on Poly(Butylene Succinate-*co*-Adipate) and Different Collagen Hydrolysates from Tanning Industry: I—Processing and Thermo-mechanical Properties

Maurizia Seggiani[1] · Roberto Altieri[2] · Patrizia Cinelli[1] · Alessandro Esposito[2] · Andrea Lazzeri[1]

Abstract

In this study, blends of a biodegradable thermoplastic polyester, poly (butylene succinate-*co*-adipate) (PBSA) with two different raw hydrolyzed collagens (HCs), derived from the tannery industry, were investigated in terms of processability, rheological, thermal and mechanical properties. HCs, obtained by alkaline (HCa) and enzymatic (HCe) hydrolysis of the solid wastes generated during the shaving of the tanned leather, were used in PBSA/HC blends, up to 20 wt% of HC, produced by melting extrusion and processed by injection molding. All the blends up to 20 wt% HCs resulted suitable for the injection molding obtaining flexible molded specimens with good tensile properties. The different secondary structure of the two HCs influenced the rheology, morphology and mechanical properties of the produced blends. In particular, HCa, due its higher content of oligopeptides and free amino-acids, showed a good compatibility with the polymeric matrix acting as a plasticizer with consequent reduction of melt viscosity with increasing its loading. The molded dog-bones specimens containing 20 wt% HCa showed a value of elongation at break of 810%. While, HCe, due its higher presence of b-sheet structures, behaved as organic filler, showing a poor interfacial interaction with PBSA with consequent decrease of the tensile properties with increasing its loading. The good processability and satisfactory mechanical properties obtained encourage the use of both investigated collagen hydrolysates in the production of thermoplastic blends and relative molded products for applications in agriculture and plant nurseries, such as pots or small containers with fertilizing properties, due the presence of HCs.

Keywords Poly (butylene succinate-*co*-adipate) · Hydrolyzed collagen · Tannery industry · Thermoplastic blends · Injection molding

Introduction

Among the commercially available biodegradable plastics, poly (butylene succinate-*co*-adipate) (PBSA) is a promising thermoplastic aliphatic polyester with many interesting properties: excellent processability in extrusion, thermoforming, film blowing and injection molding, biodegradability in different environments (industrial/home composting and soil), and good mechanical performance similar to that of polyolefins [1–6]. PBSA is a random co-polyester synthetized by the reaction of 1,4-butanediol with aliphatic dicarboxylic acids such as succinic and adipic acids, and it is commercially available in different grades (molecular weights from 10,000 to 100,000 g/mol) for various applications [1–3]. Some manufactures, such as Mitsubishi Chemical, produce partially biobased poly (butylene succinate), PBS, and PBSA having 54 wt% biobased content derived from biobased succinic acid [7], although synthetic PBS and PBSA are still the most common products on the market [8]. Compared to PBS, PBSA exhibits a higher rate of biodegradation in industrial composting and recent studies have reported that PBSA, in forms of films and molded items, results biodegradable within few months in soil, sea water and water with activated sludge [3, 4, 6–9]. PBSA shows higher impact strength and elongation, lower tensile

✉ Maurizia Seggiani
maurizia.seggiani@unipi.it

✉ Roberto Altieri
roberto.altieri@cnr.it

1   Department of Civil and Industrial Engineering, University of Pisa, Largo Lucio Lazzarino n. 2, 56122 Pisa, Italy

2   Institute for Agricultural and Forest Systems in the Mediterranean, Consiglio Nazionale Delle Ricerche, (ISAFoM-CNR), Via della Madonna Alta 128, 06128 Perugia, Italy

strength and melting point respect to PBS, due to its lower crystallinity and higher flexibility of its polymer chains [9]. For these reasons, PBSA results more attractive respect to PBS for those applications where the biodegradability in soil can become the key prerequisite such as molded plant pots and agricultural mulching films. In fact, pure PBSA films are proposed as bag liners, mulch film and agricultural films [10]. Despite these attractive properties, the use of PBSA in short-term applications is still very slowed by its relatively high cost (5–6 €/kg, info from MCCP Germany GmbH) compared to that of the petroleum-derived, non-biodegradable, plastics and also of other bioplastics, such as poly-lactic acid (PLA). So, in order for PBSA to be more attractive for commodities, the addition of low-cost biodegradable and renewable components in blend can represent a strategy to produce biodegradable PBSA-based blends with improved cost competitiveness. For this reason, PBSA has been successfully blended with corn starch [1, 11, 12] to obtain biodegradable composites with good processability and mechanical performances.

For the same purpose, also waste protein hydrolysates such as hydrolyzed collagens (HC) from tanning industry could be used in blend with PBSA given the well-known good adhesive properties of proteins and their good melt processability. Different authors have studied blends containing HC and synthetic polymers such as polycaprolactone (PCL) [13, 14], polyvinyl alcohol (PVA) [15, 16], low-density polyethylene (LDPE) [17, 18] and polyvinylchloride (PVC) [19] showing the positive effect of the HC on the blend processability by conventional melting-based processes.

The addition of HCs to PBSA can lower the cost of the final item as well as improve the biodegradability of the polymer supporting the microbial growth upon environmental exposure and give to the final product fertilizing properties given the presence of protein nitrogen. To our knowledge, only our work has been reported in scientific literature concerns preliminary encouraging results of processing the PBSA with raw hydrolyzed collagen derived by alkaline hydrolysis of leather shavings by blow-film molding [20].

Shavings along with fleshings represent the most important solid by-products of the tannery industry and are mainly constituted of raw collagen. The shaving process is carried out after tanning to reduce and/or even out the thickness throughout the tanned or crusted leather. The leathers are put through a machine with a rapidly revolving cylinder cutting fine, thin fragments from the flesh side. The small pieces of leather which are shaved off are called shavings. In Italy, such wastes derived from leather districts, such as Santa Croce sull'Arno (Pisa, Italy) and Arzignano (Vicenza, Italy) are collected and processed in centralized plants where, through alkaline or enzymatic hydrolysis, degreasing, concentration, centrifugation and, eventually, spray-drying,

collagen hydrolysates in solution or powder are produced. Actually, these hydrolysates are used as organic fertilizers in agriculture due to their relatively high nitrogen content (about 13–15 wt%) and moderate salt content. The collagen hydrolysates from the leather industry are available at low cost (1.20 €/kg powder, info by Consorzio SGS, Santa Croce sull'Arno, Pisa, Italy) and their use, unlike corn starch, is not in competition with food industries.

Thus, the present work focuses on the addition to PBSA of two different raw hydrolyzed collagens (HCs), obtained from leather shavings by different hydrolysis processes (alkaline and enzymatic hydrolysis), with the aim of developing thermoplastic biodegradable blends with improved cost competitiveness, maintaining good processability and mechanical performance.

In particular, PBSA/HC blends with 5, 10, 15 and 20 wt% of HC were produced by melt extrusion and the resultant pellets were processed by injection molding. The blends were characterized by Scanning Electron Microscopy (SEM) coupled with an energy dispersive X-ray spectrometry (EDS), by Fourier Transform Infrared (FTIR) analysis in order to evaluate the dispersibility of HCs into the polymer matrix and to evaluate the intermolecular interactions between PBSA and HCs, respectively. Furthermore, the rheological behavior of the blends was investigated to evaluate the effect of HCs on the melt viscosity and the molded dog-bone specimens were characterized by tensile tests.

Experimental

Materials

Pellets of PBSA (trade name BioPBS™ FD92PM) were purchased from MCCP Germany GmbH (Mitsubishi Chemical Co., Tokyo, Japan). FD92PM is produced by copolymerization of bio-based succinic acid and adipic acid with 1,4-butanediol [3, 20], having a melting temperature of 84 °C, density of 1.24 g/cm³, melt flow rate (MFR) of 4 g/10 min (190 °C/2.16 kg), suitable for blown film applications (i.e., bag liners, mulch film, agricultural film). FD92PM is a food contact grade in accordance with EU10/2011 and certified home compostable and biodegradable in soil by Vinçotte. Two types of hydrolyzed collagen from tannery industry were used: an hydrolyzed collagen derived from alkaline hydrolysis of shavings, labeled as HCa, supplied by Consorzio SGS SpA (Santa Croce sull'Arno, Pisa, Italy) in form of dark yellow granules, and an hydrolyzed collagen derived from enzymatic hydrolysis of shavings, HCe, supplied by ILSA S.p.a. (Verona, Italy) in white powder form. Figure 1 shows the two HCs used in this work.

The composition of the two HCs, provided by suppliers, is reported in Table 1. As shown, HCa shows higher content
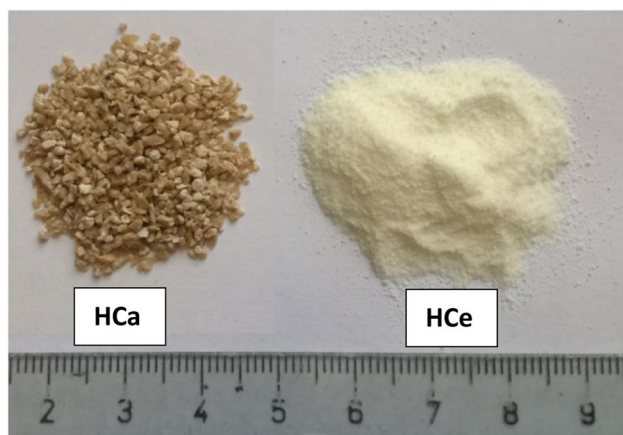
Fig. 1 Hydrolyzed collagens (HCa and HCe) used in this work

Table 1 Properties of the HCs used in preparation of PBSA/HC blends

Property	HCa	HCe
Dry matter (at 103 °C, wt%)	97.0	99.9
Ash (at 550 °C, wt% db)	7.3	<1
Bulk density (kg/L)	0.50	0.55
Total nitrogen (wt% db)	14.1	15.9
Organic nitrogen (wt% db)	13.2	15.9
Organic carbon (wt% db)	43.7	49.5
Organic matter (wt% db)	87.4	99.0
NaCl content (wt% db)	7.8	<1
Total amino acids (wt% db)	88.9	99.0
Free amino acids (wt% db)	39.7	0.6
pH in aqueous solution	5.3	6.1
Water solubility (1:4, w/v)	Total	Almost total

db dry basis

(about 40 wt% on dry basis) of free aminoacids compared to HCe (below 1 wt%). Both HCs, being highly hydrophilic, in particular HCa, were dried under vacuum at 50 °C for 24 h before use.

Blend Production and Processing

PBSA/HC blends were prepared by melting extrusion in a semi-industrial twin screw extruder, a Comac EBC 25 HT (Comac, Milan, Italy), feeding dried pellets of the pure PBSA in the main feeder hopper and the granules/powders of HCa and HCe by a side-feeder in adequate weight ratios to obtain blends with 5, 10, 15 and 20 wt% HC, respect to the total weight, labeled as PHa5, PHe5, PHa10, PHe10, PHa15, PHe15, PHa20, PHe20, respectively. The temperature profiles set in the extruder (from the first zone after the main feeder to the head zone) for the PBSA/HC blends are reported in Table 2 with the temperature and pressure of the melt measured at the nozzle exit of 125 °C and 12 atm, respectively, for the PHa blends and 133 °C and 25 atm for the PHe blends. The screw speed was 250 rpm for both blends. The extruded filaments were cooled in a water bath at room temperature and reduced in pellets by a pelletizing unit equipped with rotating blades. The pellets, after drying at 60 °C for 12 h in a Piovan dryer (DP 604–615, Piovan, Venezia, Italy), were processed in an injection press (model Mega Tech H10/18–1, Tecnica Duebi srl, Ancona, Italy) to produce specimens (Haake III type dog-bone tensile bars: width 10 mm, width in the narrow Sect. 4.8 mm, thickness 1.35 mm, length 90 mm) used for the tensile tests (Fig. 2) and disintegration tests carried out by Altieri et al. [21] under controlled composting conditions at different temperature (58 and 25 °C), according to international standards. In the injection press the temperature profile in the three zones was 125, 135 and 145 °C, mold temperature of 15–25 °C, injection and post pressure of 20–25 and 20–35 bar, respectively, and cycle time of 30 s.

In addition, the pellets were also used to produce sheets with thickness of 200–300 μm by a lab hot press (model 10 T press, NOSELAB ATS s.r.l, Nova Milanese (MB), Italy) at 170 °C. The hot-pressed films were used in the disintegration tests under simulated composting conditions reported by Altieri et al. [21].

Characterization

Thermogravimetric Analysis

Thermogravimetric analysis (TGA) was performed on the starting materials (PBSA, HCa and HCe) and the PBSA/HC blends in form of pellets by a TA Q-500 (TA Instruments, Waters LLC, New Castle, DE, USA). About 15 mg of sample were loaded into a platinum pan and heated from room temperature to 800 °C at 10 °C/min under nitrogen atmosphere. TGA was used to evaluate the thermal stability of the different used HCs in view of their processing by

Table 2 Temperature profiles adopted in the extruder for the different PBSA/HC blends

	Feed										Head
Blends	T_1 (°C)	T_2 (°C)	T_3 (°C)	T_4 (°C)	T_5 (°C)	T_6 (°C)	T_7 (°C)	T_8 (°C)	T_9 (°C)	T_{10} (°C)	T_{11} (°C)
PHa	155	165	165	160	160	160	160	160	160	165	170
PHe	155	170	170	170	170	165	165	165	165	170	170

Fig. 2 Tensile dog-bone specimens of PBSA and PBSA/HC blends
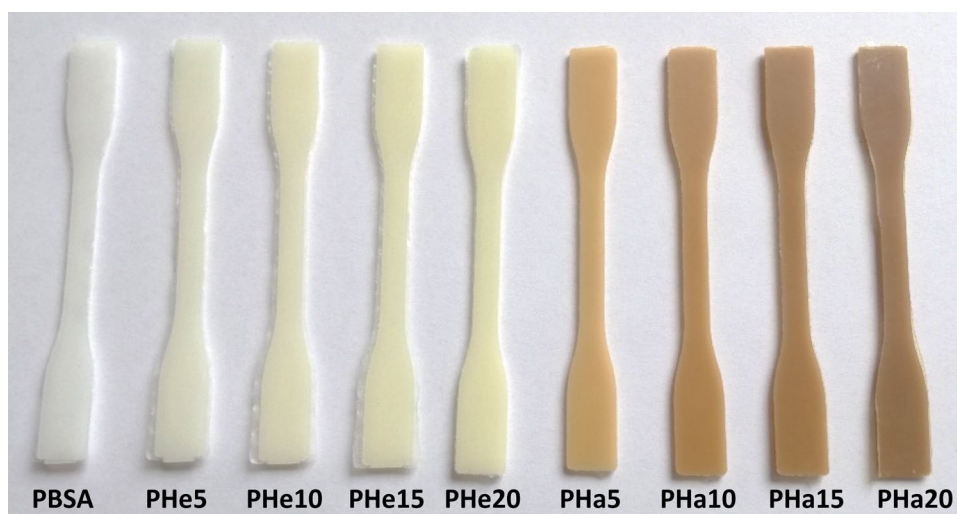
melting extrusion with PBSA and the effect of HCs on the thermal behavior of PBSA.

Differential Scanning Calorimetry

Differential scanning calorimetry (DSC) was carried out on the HCs and blend pellets by a Perkin Elmer Pyris 1 (Perkin Elmer Instrument, Waltham, MA, U.S.) under nitrogen flow (50 mL/min). About 25 mg of pellets were put in a hermetically sealed aluminum pan and subjected to first heating/cooling/second heating at 10/20/10 °C/min, respectively, beginning with heating from 20 to 150 °C (to remove any thermal history from processing), cooling to 0 °C, and subsequently heating to 150 °C. The melting temperature (T_m) and enthalpy (ΔH_m) were determined by the second heating DSC data and used to evaluate the crystallinity χ_c of PBSA by the Eq. (1):

$$\chi_c(\%) = \frac{\Delta H_m}{\Delta H_m^0 \cdot f_w} 100\% \tag{1}$$

where ΔH_m^0 is the melting enthalpy per gram of the 100% crystalline PBSA (142 J/g; [22]), and the f_w is the weight fraction of PBSA in the blend.

Fourier Transform Infrared (FTIR) Analysis

FTIR spectroscopy was used to investigate the primary and secondary structure of the used HCs and the possible intermolecular interactions occurred between the functional groups of HCs and those of PBSA. FTIR spectra were recorded on a Perkin Elmer Spectrum One FT-IR Spectrometer (Perkin Elmer, Waltham, MA, USA), equipped with a Perkin Elmer Universal ATR Sampling Accessory,

in the wavenumber range of 4000–650 cm^{-1} at 4 cm^{-1} scanning resolution. FTIR spectroscopy was carried on the HCs in form of powder and on the pellets of neat PBSA and PBSA/HC blends. All the samples were pre-dried at 40 °C in a vacuum oven for 24 h before the FTIR analysis.

Mechanical Tests

Tensile properties of injection molded Haake III Type (557–2290) dog-bone specimens of neat PBSA and PBSA/HC blends were evaluated in accordance with ASTM D 638 using an Instron 5500R tensiometer (Instron, Norwood, MA, USA), equipped with a 1 kN load cell. The tensile tests were carried out at room temperature with a crosshead speed of 10 mm/min. For each sample, at least 5 replicates were carried out.

Rheological Properties

In order to evaluate the effect of the different used HCs on the fluidity of the melt PBSA/HC blends, the Melt Flow Rate (MFR) and Melt Volume Rate (MVR) measurements were carried out according to UNI EN ISO 1133 by a Ceast Melt Flow Tester MF20 (Instron, Canton, MA, USA) equipped with automatic weight lifting and cutting systems. MFR and MVR represent the amount of melt polymer, expressed in mass (grams) and volume (cm^3), respectively, flowing per 10 min through a capillary of specific diameter and length under a pressure applied at a specified temperature. 4.5 g of sample pellets were heated at 150 °C in the barrel and extruded through the normalized die (diameter 2.095 mm) under a constant load of 2.16 kg. MFR and MVR of PBSA and PBSA/HC blends were measured and the melt density was evaluated by the ratio MFR/MVR.

In addition, the melt rheological measurements were carried out by an MCR 92 Rheometer (Anton Paar Italia, Rivoli, Italy) using a plate-plate geometry (25 mm diameter, 2 mm gap) in the temperature range of 130–160 °C. Sample in form of pellets was used for each run and a waiting time of 3 min was applied for each test. All the samples were dried before testing and for each sample, 3 replicates were carried out.

Scanning Electron Microscopy

Neat PBSA and PBSA/HC pellets were fractured in liquid nitrogen and the fracture surfaces were observed by scanning electron microscopy (SEM) using a Quanta FEG 450 (FEI Inc.) coupled to an energy dispersive X-ray spectrometer (EDS). EDS microanalysis was also conducted to obtain information on the dispersion of the different HC in the PBSA matrix, since HCs contain salts such as NaCl (Table 1). Before the SEM analysis, the fractured sections were coated with a homogeneous layer (5–6 nm thickness) of Au by a SEM coating device (Edward Spotter Coater) to induce electroconductivity.

Results and Discussion

Processing

The PBSA/HC blends containing up to 20 wt% HCs did not show any problem during the extrusion process showing that the addition of HCs to the PBSA did not compromise its processability. While, during the injection molding, the extrusion and mold temperatures were slightly reduced with the increasing the HC content to compensate the increase of blend fluidity for HCa and to reduce the possible development of volatile compounds that lead to molding volume contraction with consequent formation of localized sink marks on the specimen surface. Figure 2 shows some of the dog-bone specimens produced from neat PBSA and PBSA/HC blends. As shown, the dog-bones containing HCe appear slightly yellow, while those containing HCa caramel; the color becomes more intense with increasing the HC content.

Thermal Properties

Thermogravimetric (TG) curves as a function of temperature of HCs, PBSA and PBSA/HC blends are shown in Fig. 3. HCs, after initial residual moisture loss, particularly evidenced in HCa, due to its higher hydrophilicity than HCe, presented a further weight loss in the range 150–200 °C related to the loss of low molecular oligopeptides, and then

**Fig. 3** TG curves of HCs, PBSA and PBSA/HC blends under inert atmosphere
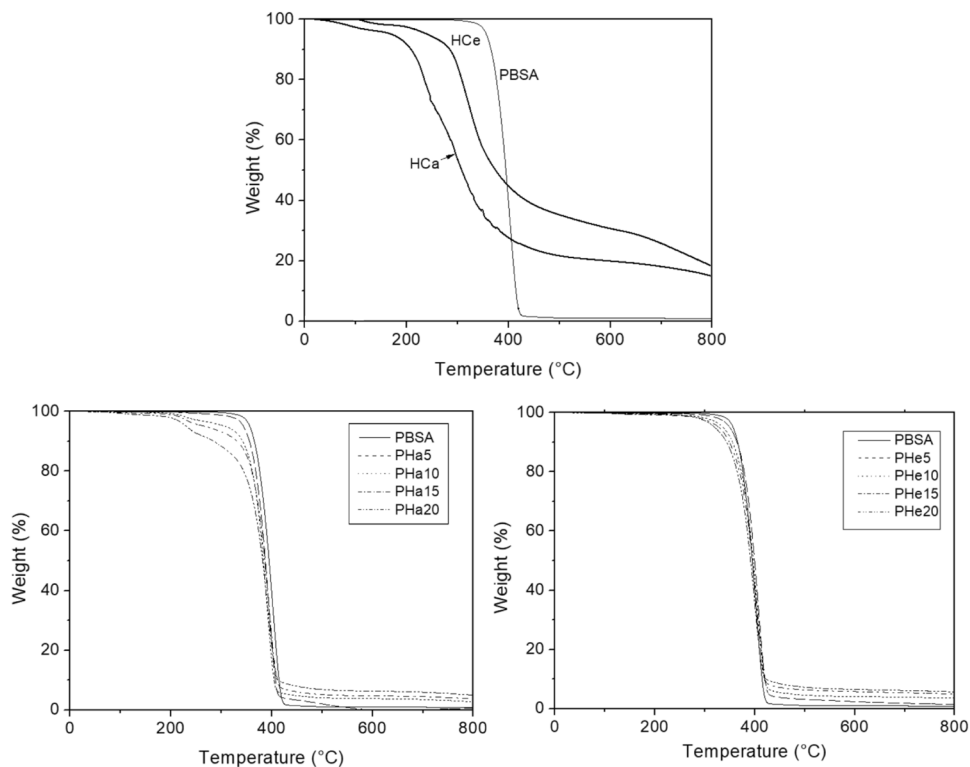
a major weight loss in the range 200–400 °C. The amplitude of this decomposition temperature range is attributable to the distribution of the lengths of the peptide chains and free amino acids. HCe resulted thermally more stable than HCa showing the thermal degradation curve shifted to higher temperatures (Fig. 3). Furthermore, HCa presented a higher residual weight a 800 °C than HCe as expected because of higher content of salts in HCa (Table 1). The TG curve of PBSA showed thermal stability up to 300 °C and, then, a single-stage thermal degradation with peak close to 400 °C. A negligible residue (0.3%) was observed at 800 °C.

The TG curves of the blends derived from the combined effect of the two components, the weight loss in the range 200–250 °C, more evident in PHa blends, is attributable to the thermal degradation of the HC in the blend and the subsequent weight loss to the concomitant thermal degradations of HC and PBSA showing that no significant variation of the thermal stability of PBSA was observed when HC was incorporated to the polymeric matrix. Thus, the thermal stability of both HCs up to 150–160 °C attests their suitability to be processed with thermoplastic polymers having extrusion temperatures below these values such as PBSA without incurring thermal degradation. In addition, given the high hydrophilicity of HCs, in particular HCa, it is necessary to dry them before being processed with PBSA to avoid the development of water vapor during extrusion phase. Differential scanning calorimetry (DSC) was used to investigate the effect of the two HCs on the crystallization behavior of PBSA. The 1st heating scan was omitted and the analyses were focused on the second heating to eliminate any possible interference of the previous thermal history. The DSC curves obtained during the 2nd heating of the HCs, PBSA and the PBSA/HC blends containing 20 wt% of HC are reported in Fig. 4.

The melting temperature/s (T_m), the melting heat (ΔH_m) normalized to PBSA content, and the PBSA crystallinity index are summarized in the Table 3.

As shown, the neat PBSA and the blend PHa20 show a single endothermic peak at 88 and 87 °C, respectively; while PBSA shows two melting peaks in the blend PHe20: the first peak at 75 °C and the second one at 87 °C. This shows that the presence of HCe leads to the formation of two crystalline phases of PBSA, one that melts at a temperature lower than that of neat PBSA and the other at the same temperature of the neat PBSA. The total fusion heat (ΔH_m), evaluated by integration of the area under the two melting peaks of PBSA and normalized to PBSA content, decreased slightly in the PHe20 blend as the crystallinity index; while in the PHa20 blend a marked reduction of ΔH_m was observed leading to a reduction of the degree of crystallinity of PBSA from 31 to 19%, as shown in Table 3. Consequently, on the basis of these results, HCe appeared to hinder the crystallization of PBSA while HCa had a negligible effect.
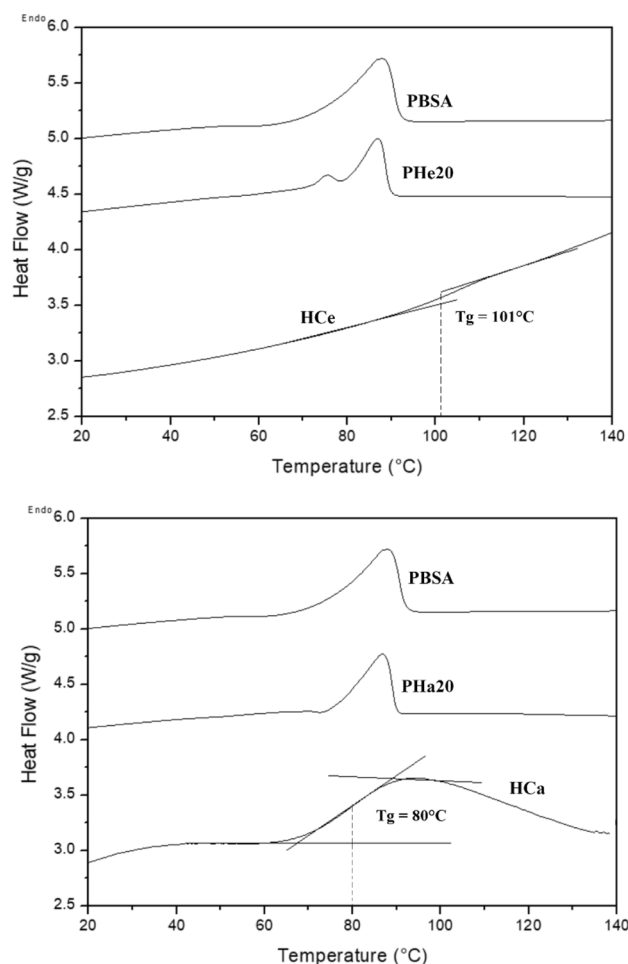
Fig. 4 DSC curves of PBSA, HCs and the PBSA/HC blends with 20 wt% HC during the 2nd heating

Table 3 Thermal parameters and crystallinity index of PBSA and its blends with 20 wt% HC

| Sample	T_{m1} (°C)	T_{m2} (°C)	ΔH_m (J/g)	χ_c
PBSA	–	88.0	36.6	31.3
PHe20	75.4	87.0	22.5	19.2
PHa20	–	86.8	33.0	28.2

FTIR Analysis

The FTIR spectra of neat PBSA, HCs, PHa20 and PHa20 blends and the second derivative spectra of the HCs are reported in Figs. 5 and 6, respectively.

As shown, the spectra of HCs show the typical peaks of amide A, B, I, II and III (about 3300, 3070, 1650, 1550 and 1300 cm^{-1}, respectively [23]). FTIR spectra peaks of PBSA located at 1714 and 1153 cm^{-1} are assigned to C=O and C–O, respectively. No relevant reaction seemed to take
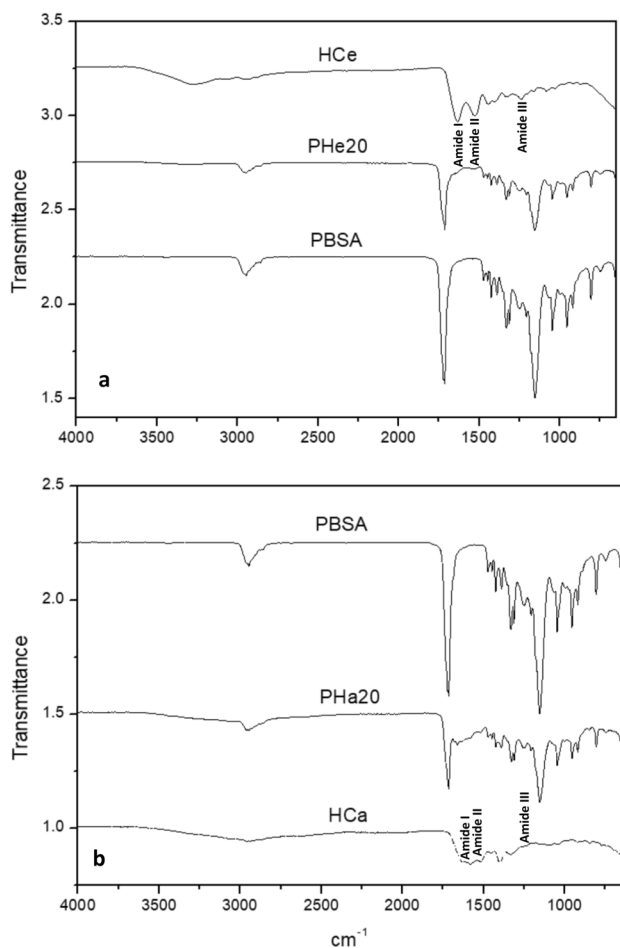
Fig. 5 FTIR spectrum of **a** neat PBSA, HCe and PHe20; and **b** neat PBSA, HCa and PHa20
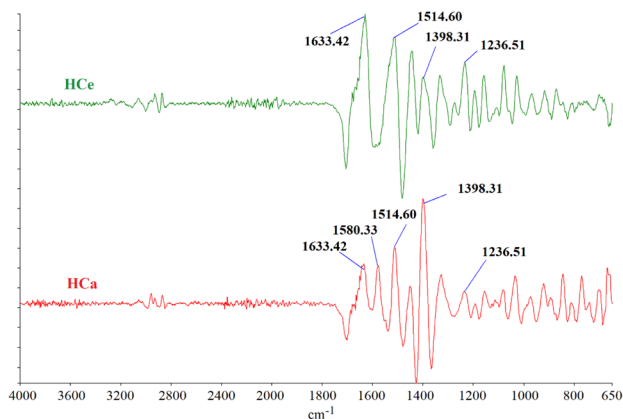
Fig. 6 Second derivative FTIR spectra of the used HCs

place between the PBSA and the collagen hydrolysates: the blend spectrum resulted an overlapping of the typical peaks of the pure components.

The second derivative of FTIR spectra (Fig. 6) shows the differences between the secondary structures of the two used HC. The second derivative spectra clearly resolved peaks that are associated with α-helix, β-strands and turns.

In this case, in both HCs the absence of the peak near to 1650 cm^{-1} indicates no α-helix structures [23]. While, the peak at 1633.42 cm^{-1} is attributable to β-sheet conformations [23], and the more intense peak in HCe indicates a higher proportion of β-sheet structures compared to HCa. In addition, the peak observed in HCa at 1580 cm^{-1} is attributable to carboxylates (carboxylic acid salts) due to the presence of oligopeptides or free amino-acids.

In conclusion, as expected, the alkaline hydrolysis resulted more destructive than enzymatic hydrolysis, carried out using exo-endo proteases. For this reason, in the HCa there is a significant proportion of oligopeptides and free amino acids together with β-sheet structures. This is confirmed also by the analysis reported in Table 1.

Rheological Properties

Melt fluidity measurements of the PBSA neat and PBSA/HC blends are reported in Fig. 7 in terms of MFR and MVR values obtained at 150 °C. As shown, addition of HCa decreased significantly the melt viscosity at low shear rate, the MFR and MVR values increased almost linearly with increasing HC content. This marked decrease of viscosity can be attributed to the alignment of the small chains of HCa in neighboring macromolecules of PBSA that improves the chain movement with consequent reduction of the melt viscosity. Consequently, HCa appeared to act as plasticizer due to its good lubrication characteristics which promoted the interphase slip. For content below 15 wt%, as evidenced
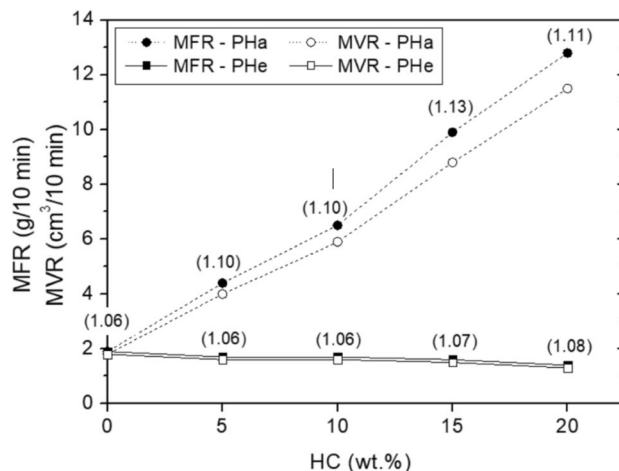

Fig. 7 MFR and MVR values obtained at 150 °C for neat PBSA and PBSA/HC blends; the values in brackets represent the melt density in g/cm^3 evaluated by the MFR/MVR ratio

by the morphological analysis, HCa resulted homogeneously dispersed into the polymeric matrix, while above 15 wt% the presence of macrodomains of HCa were observed. Consequently, the further increase of MFR and MVR values for high HCa contents can be attributable to the lubricant effect of HCa along the barrel walls that facilitated the sliding of the molten material.

As shown in Fig. 7, a totally different behavior was observed for the PBSA/HC blends containing HCe. For these blends, the melt fluidity decreased slightly with increasing the HCe content. As observed by morphological analysis, the powder of HCe appeared homogeneously dispersed in the blend but the weaker interfacial interactions between HCe and PBSA and the lower lubricant capacity of HCe compared with those of HCa led to a reduction of polymer chain mobility with increasing the content of HCe particles which perturb the normal flow and hinder the mobility of chain segments in melt flow, consequently decreasing the blend fluidity. This rheological behavior is typical of the filled polymer composites where the melt viscosity increases with increasing filler content [24, 25]. Therefore, HCe resulted to act as filler in the blend as evidenced also by the SEM analysis and by observations with the naked eye carried out on the PBSA/HCe films and dog bone specimens.

As example, Fig. 8 show the complex viscosity vs frequency for the neat PBSA and PBSA/HC blends obtained at 130 and 150 °C. As expected, the complex viscosity decreased with increasing the temperature and decreased with increasing the frequency, showing a non-Newtonian fluid behavior over entire frequency range with a characteristic shear thinning [26–28]. At the investigated temperatures and in the frequency range that coincides with the characteristic frequencies of the extrusion process (1–1000 rad/s, TA Instrument application note [29]), the blends containing HCa showed lower viscosities compared to the neat PBSA, while the blends with HCe higher viscosities. This trend confirms the plasticizing effect of HCa and the filler effect of HCe: the melt viscosity decreased with increasing the HCa while it increased with increasing the HCe content.
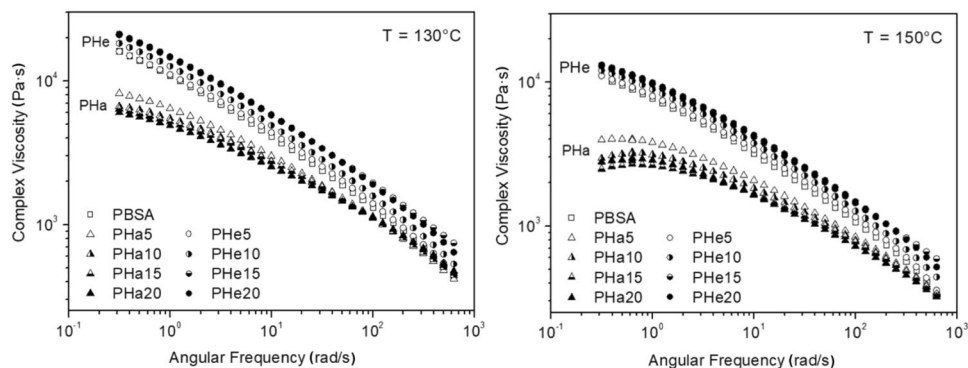
Morphological Analysis

As example, Fig. 9 show the SEM images of the cross-sections of the pellets of PBSA and PBSA/HC blends containing 10 and 20 wt% of HC. In addition, to investigate the dispersion of HCs in the PBSA matrix, SEM–EDS microanalysis was performed given that HCs contain nitrogen and salts (see Table 1) as sodium chloride, NaCl (deriving from the raw hide salting), unlike PBSA. As example, the SEM–EDS analysis performed on the PHe10 and PHa20 pellet is reported in Figs. 10 and 11, respectively. As shown in Fig. 9b, c, the blends PHe10 and PHe20 show two distinct phases: the disperse phase, attributable to the HCe as confirmed by the SEM–EDS analysis (Fig. 10), appears as spheroid particles dispersed in the continuous phase of PBSA. Poor cohesion is shown between the two phases, indicating poor interactions between HCe and PBSA (the HC particles resulted separate from the matrix). In the blends containing HCa (Fig. 9d, e), HC resulted homogeneously dispersed into the polymeric matrix showing a good compatibility with PBSA. In the PHa10 no evident phase separation is observable; while in the PHa20 micro-domains of HC are uniformly distributed in the sample. As shown by the SEM–EDS analysis (Fig. 11), it is not possible to identify on a microscopic scale zones consisting only of PBSA or only of HCa. It is to be pointed out that the density of HC is much lower than that of PBSA (0.55 g/cm^3 (Table 1) vs 1.24 g/cm^3 of PBSA), so the percentage by volume of HC in the blend is much higher than that in mass, about twice (20 wt% corresponds to about 40 vol.%). Despite this, no macro domains of HCa are observed in the continuous phase.

Mechanical Properties

The tensile properties of the dog-bone specimens are reported in Table 4. As shown, the Young's modulus decreased with increasing HCa loading showing a softening effect induced by HCa, in particular for high HC contents. Stress–strain curves of the PBSA/HCa blends were

Fig. 8 Complex viscosity versus frequency of PBSA and PBSA/HC blends at 130 and 150 °C

Fig. 9 SEM images of the fractured transversal sections of **a** neat PBSA (2000X), **b** PHe10 (500X, 2000X), **c** PHe20 (500X, 2000X); **d** PHa10 (2000X) and **e** PHa20 (2000X) pellets
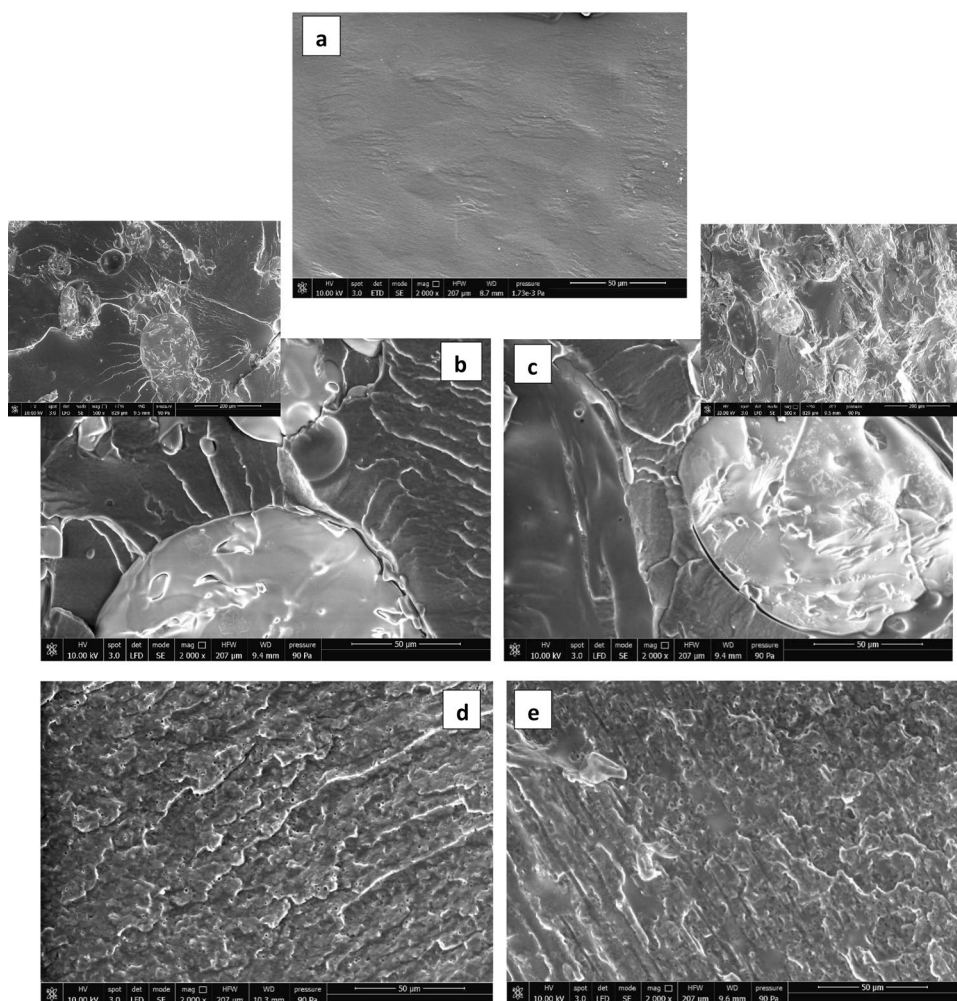

characterized by a yield strength similar to that of neat PBSA but at higher elongation; the stress at break decreased with increasing of HCa content while the elongation at break resulted higher or similar to that of neat PBSA. For the blends PBSA/HCe, a gradual increase in the Young's modulus was induced by the addition of HCe, showing its stiffening effect. According to the increase of rigidity, the elongation at break showed a marked decrease also at low percentage of HCe (5 wt.). These results are in accordance with those obtained by Dascălu et al. [18] because of poor adhesion between LDPE and HC. In conclusion, the blends PBSA/HC with HCe produce a more rigid structure compared to the blends with HCa confirming the plasticizing effect of HCa and the filler effect of HCe.

Conclusions

Blends of PBSA and two different raw hydrolyzed collagens from leather shavings were successfully processed by extrusion and injection molding up to a content of 20 wt% HC. HCs thermal stability was compatible with the melt processing of PBSA. The different secondary structure of the two HCs investigated influenced the rheological behavior of the molten blend and the mechanical performance. The HC obtained by alkaline hydrolysis (HCa) showed a good compatibility with PBSA, as evidenced by the morphological analysis, and acted as plasticizer with consequent reduction of the melt viscosity making the PBSA/HC blend softer. While the collagen hydrolysate obtained by enzymatic hydrolysis (HCe) showed lower compatibility with the polymeric matrix and behaved as a filler making the blends little more rigid with the increasing of its content in the blend.

The molted dog-bone specimens of both blend series showed good flexibility and satisfactory mechanical

Fig. 10 SEM–EDS microanalysis performed on the cross-sections of PHe10 pellet
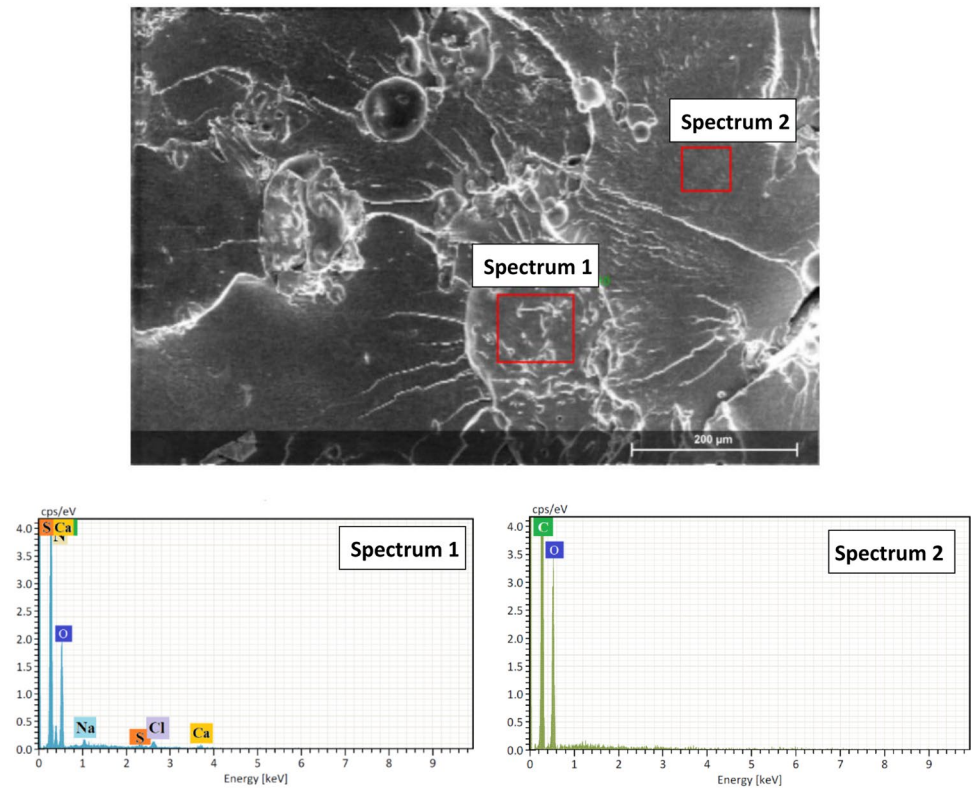
Fig. 11 SEM–EDS microanalysis performed on the cross-sections of PHa20 pellet
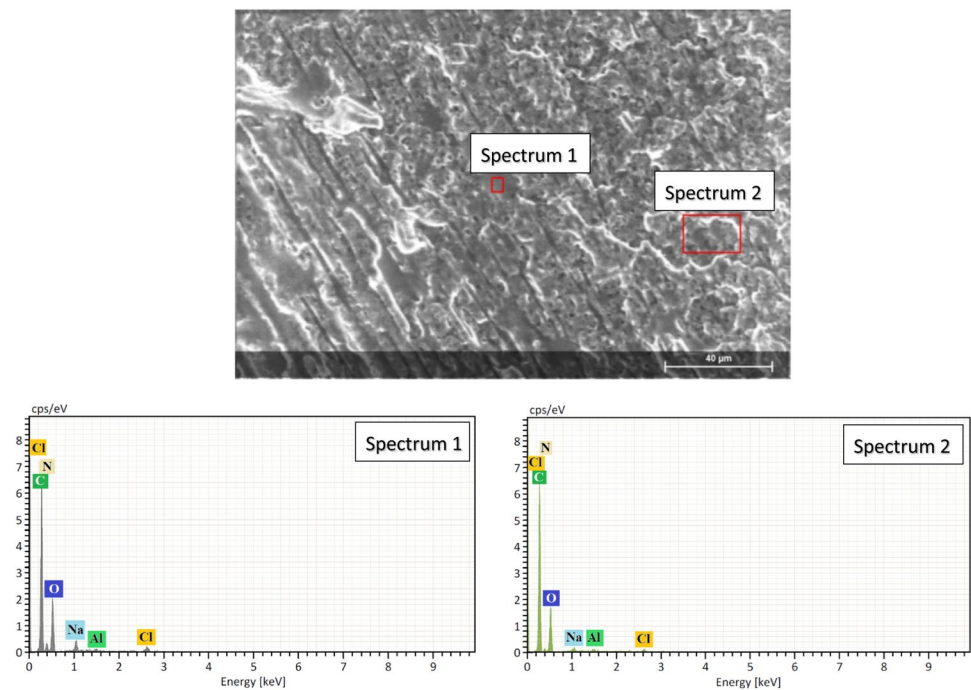
properties in the absence of crosslink agent and/or compatibilizing agents.

In conclusion, PBSA matrix showed a good capability to incorporate the two different investigated HCs without compromising its melt processability up to 20 wt% of HC and the developed PBSA/HC blends appear promising candidates for the production of biodegradable/compostable items such as plant molded plots having fertilizing

Table 4 Mechanical properties of the tensile PBSA and PBSA/HC specimens

Sample	Young's modulus (GPa)	Yield strength (MPa)	Elongation at yield (%)	Stress at break (MPa)	Elongation at break (%)
PBSA	0.32 ± 0.01	17.5 ± 1.3	20.1 ± 1.3	28.4 ± 2.1	776.0 ± 24.8
PHa5	0.29 ± 0.03	14.8 ± 0.3	24.1 ± 0.3	23.7 ± 0.6	715.1 ± 35.5
PHa10	0.13 ± 0.06	13.5 ± 0.2	27.5 ± 0.2	23.6 ± 0.4	805.3 ± 29.1
PHa15	0.12 ± 0.04	12.8 ± 1.1	34.1 ± 1.1	20.1 ± 1.0	802.5 ± 46.2
PHa20	0.10 ± 0.01	12.2 ± 0.7	28.2 ± 0.7	11.7 ± 2.1	809.9 ± 68.1
PHe5	0.37 ± 0.08	16.0 ± 0.3	16.0 ± 0.3	21.9 ± 2.1	225.0 ± 10.2
PHe10	0.39 ± 0.01	15.2 ± 0.8	10.1 ± 0.8	20.1 ± 1.7	187.5 ± 12.5
PHe15	0.38 ± 0.03	12.4 ± 1.2	13.2 ± 1.2	18.1 ± 1.1	131.2 ± 10.7
PHe20	0.43 ± 0.08	13.5 ± 1.3	9.9 ± 1.3	20.0 ± 0.9	102.5 ± 21.1

Mean values $\pm$ standard deviation of 5 replicates

properties, given the presence of HC, for applications in agriculture and represent an opportunity for valorizing these by-products of the tanning industry in the bioplastic sector.

References

1. Ratto JA, Stenhouse PJ, Auerbach M, Mitchell J, Farrell R (1999) Polymer 40:6777. https://doi.org/10.1016/S0032-3861(99)00014-2
2. Ishioka DR, Kitakuni E, Ichikawa Y (2002) Aliphatic polyesters: bionolle. Bipolymers, polyesters III. Wiley, New York
3. Fujimaki T (1998) Polym Degrad Stab 159:209. https://doi.org/10.1016/S0141-3910(97)00220-6
4. Mitchell M, Ryder T, Hirt D (2017) Degradation of PBSA in water, SPE ANTEC Anaheim. 482.
5. Takiyama E, Fujimaki T, Seki S, Hokari T, Hatano Y (1994) Method for manufacturing biodegradable high molecular aliphatic polyester, US Patent 5,306,787.
6. Nishioka M, Tuzuki T, Wanajyo Y, Oonami H, Horiuchi T (1994) Stud Polym Sci 12:584. https://doi.org/10.1016/B978-0-444-81708-2.50069-5
7. Zini E, Scandola M (2011) Polym Compos 2:1905. https://doi.org/10.1002/pc.21224
8. Phua YJ, Pegoretti A, Araujo TM, Ishak ZAM (2015) J Appl Polym Sci 132:42815. https://doi.org/10.1002/app.42815
9. Muthuraj R, Misra M, Mohanty AK (2015) 5—Studies on mechanical, thermal, and morphological characteristics of biocomposites from biodegradable polymer blends and natural fibers, biocomposites—design and mechanical performance. Woodhead Publ Ser Compos Sci Eng. https://doi.org/10.1016/B978-1-78242-373-7.00014-7
10. Kasirajan S, Ngouajio M (2012) Agron Sustain Dev 32:501. https://doi.org/10.1007/s13593-012-0132-7
11. Steeves DM, Farrell R, Ratto JA (2007) J Biobased Mater Bioenergy 1:94. https://doi.org/10.1166/jbmb.2007.011
12. Wang X-L, Yang K-K, Wang Y-Z (2003) J Macromol Sci Part C 43:385. https://doi.org/10.1081/MC-120023911
13. Seggiani M, Altieri R, Puccini M, Stefanelli E, Esposito A, Castellani F, Stanzione V, Vitolo S (2018) Polym Degrad Stab 150:13. https://doi.org/10.1016/j.polymdegradstab.2018.02.001
14. Vitolo S, Puccini M, Seggiani M, Castiello D (2016) Thermoplastic polymer composition, Patent: WO 2016035021 A1.
15. Chiellini E, Cinelli P, Ilieva VI, Ceccanti A, Alexy P, Bakos D (2003) Macromol Symp 197:125. https://doi.org/10.1002/masy.200350712
16. Crivoi F, Stefan L, Moldovan L, Vasile C (2009) J Optoelectron Adv Mater 11:356
17. Castiello D, Chiellini E, Cinelli P, D'Antone S, Puccini M, Salvadori M, Seggiani M (2009) J Appl Polym Sci 114:3827. https://doi.org/10.1002/app.31000
18. Dascălu MC, Vasile C, Silvestre C, Pascu M (2005) Eur Polym J 41:1391. https://doi.org/10.1016/j.eurpolymj.2004.12.005
19. Lungu M, Pascu MC, Bumbu GG, Darie H, Vasile C, Moldovan L (2004) Int J Polym Mater 53:525. https://doi.org/10.1080/00914030490267636
20. Japan BioPlastics Association. https://www.jbpaweb.net/english/e-gp-products.htm. Accessed 16 May 2020
21. Altieri R, Seggiani M, Cinelli P, Esposito A, Stanzione V (2020) Thermoplastic blends based on poly(butylene

succinate-*co*-adipate) and different collagen hydrolysates from tanning industry—II: aerobic biodegradation and compostability. J Polym Environ.

22. Pradeep SA, Kharbas H, Turng L-S, Avalos A, Lawrence JG, Pilla S (2017) Polymers 9(1):22. https://doi.org/10.3390/polym9010022

23. Barth A (2007) Biochem Biophys Acta 1767:1073. https://doi.org/10.1016/j.bbabio.2007.06.004

24. Móczó J, Pukánszky B (2017) Particulate fillers in thermoplastics. In: Rothon R (ed) Fillers for polymer applications. Polymers and polymeric composites: a reference series. Springer, Cham

25. Hornsby P (2017) Compounding of particulate-filled thermoplastics. In: Rothon R (ed) Fillers for polymer applications. Polymers and polymeric composites: a reference series. Springer, Cham

26. Li H, Huneault MA (2007) Polymer (Guildf) 48:6855. https://doi.org/10.1016/j.polymer.2007.09.020

27. Gui Z, Wang H, Gao Y, Lu C, Cheng S (2012) Iran Polym J 21:81. https://doi.org/10.1007/s13726-011-0009-7

28. Chen R, Zou W, Zhang H, Zhang G, Yang Z, Jin G, Qu J (2015) Polym Test 42:60. https://doi.org/10.1016/j.polymertesting.2015.01.015

29. Franck A (2004) Understanding rheology of thermoplastic polymers. TA Instruments. p. 1–8.